13th International Symposium on Turbulence and Shear Flow Phenomena (TSFP13)
Montreal, Canada, June 25–28, 2024

REDUCING DRAG IN TURBULENT PIPE FLOW BY AZIMUTHAL WALL OSCILLATION

Lena F Sabidussi
Department of Mechanical and Aerospace Engineering
Princeton University
Princeton, NJ 08540 USA
lenas@princeton.edu

Liuyang Ding
Department of Mechanical and Aerospace Engineering
Princeton University
Princeton, NJ 08540 USA
liuyangd@princeton.edu

Marcus Hultmark
Department of Mechanical and Aerospace Engineering
Princeton University
Princeton, NJ 08540 USA
hultmark@princeton.edu

Alexander J Smits
Department of Mechanical and Aerospace Engineering
Princeton University
Princeton, NJ 08540 USA
asmits@princeton.edu

ABSTRACT

An oscillating pipe flow experiment is performed to examine drag reduction behavior in high Reynolds number flows. A novel experimental set-up allows for a large range of oscillation amplitudes, frequencies, and friction Reynolds numbers (ranging from 856 to 5744). A maximum drag reduction of 31% is reported. The results support the suggestion that the key scaling parameter is the non-dimensional acceleration of the surface oscillation, which collapses all the data regardless of Reynolds number, actuation frequency, and actuation amplitude. This scaling holds for non-dimensional periods of oscillation down to approximately 100, which corresponds to the value that is commonly proposed to achieve the maximum level of drag reduction.

INTRODUCTION

New methods to reduce turbulent drag will enable enhanced operational efficiency and energy conservation across industrial applications like wind turbines, oil pipelines, airplanes, and marine vessels. One promising method to achieve significant turbulent drag reduction at Reynolds numbers relevant to these industrial applications is to use transverse momentum injection (TMI) created by streamwise traveling waves of spanwise wall oscillations. This mechanism, shown in figure 1, uses wall oscillations described by:

$$w(x,t) = A\sin(\kappa_x x - \omega t), \tag{1}$$

Here $w(x,t)$ is the instantaneous spanwise velocity of the wall, A is the amplitude of the spanwise velocity, κ_x is the streamwise wavenumber of the traveling wave, ω is the spanwise angular frequency, x is the location in the streamwise direction, and t is time (Quadrio *et al.*, 2009).

Transverse momentum injection has been widely studied at low Reynolds numbers, that is, for $Re_\tau < 1000$, where the friction Reynolds number $Re_\tau = u_\tau R/\nu$ (u_τ is the friction velocity, ν is the fluid kinematic viscosity, and R denotes the pipe radius, channel half height or boundary layer thickness).

Studies with $Re_\tau < 500$ fall below the "fully turbulent" regime as defined by Lee & Moser (2015); however, drag reduction up to 50% has been reported at these very low Reynolds numbers (Gatti & Quadrio, 2016). For $500 < Re_\tau < 1000$, computations for turbulent channel flow show that TMI can reduce drag by around 40% in this range when an optimal wavelength and frequency of actuation are chosen (Gatti & Quadrio, 2016, 2013; Hurst *et al.*, 2014). Related experimental work typically reports somewhat lower drag reduction (Bird *et al.*, 2018; Wu, 2000; Choi & Graham, 1998), although Choi *et al.* (1998) demonstrated drag reduction up to 45% at $Re_\tau = 549$ in a boundary layer in the absence of a traveling wave ($\kappa_x = 0$).

In addition to this work, a limited number of numerical simulations have been performed at moderate Re_τ values up to about 2000. These result in a maximum drag reduction of 37% in the case of a traveling wave ($\kappa_x > 0$), and 23% in the case of no traveling wave ($\kappa_x = 0$) (Gatti & Quadrio, 2013 and Yao *et al.*, 2019, respectively). The maximum drag reduction was typically found at an actuating frequency corresponding to the non-dimensional time constant $T^+ = 2\pi u_\tau^2/(\nu\omega) \approx 100$.

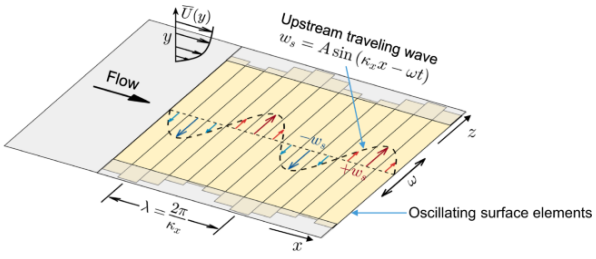

Figure 1. Schematic from Marusic *et al.* (2021) of streamwise traveling waves of spanwise oscillating wall panels.

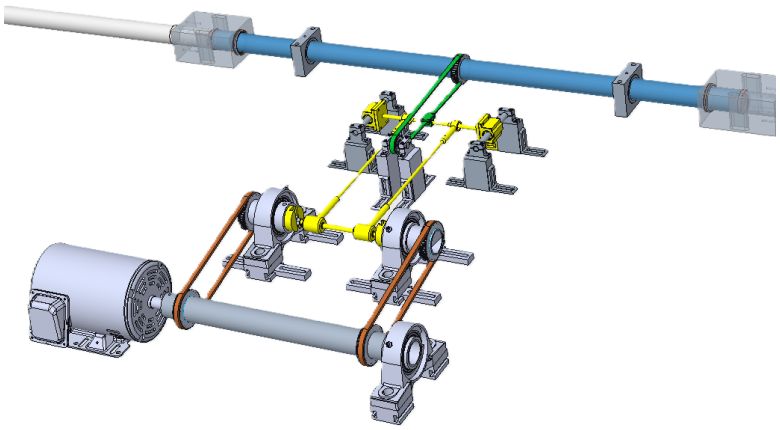

Figure 2. Model of the pipe test section. The pipe test section (in blue) is connected to a crank-slider mechanism (in yellow). The crank includes symmetrical T-slot connections attached to the motor via two timing belts (in orange). Linear motion of the crank-slider mechanism is converted to oscillatory motion via an additional timing belt (in green).

More recently, Marusic *et al.* (2021) performed experiments using TMI in a boundary layer at Reynolds numbers up to $Re_\tau = 12{,}800$, while covering a wide range of T^+ and $A^+ = A/u_\tau$. They distinguished two broad regimes for drag reduction. For $T^+ < 350$, they argued that the actuation targeted the near-wall motions, and they called this inner-scaled actuation (ISA). Although ISA can produce significant levels of drag reduction, it becomes more difficult to achieve net power savings as the Reynolds number increases because the necessary actuation frequency increases at the same time. The regime for $T^+ > 350$ was identified as outer-scaled actuation (OSA), in that it was believed to target the large-scale, outer-layer motions. Significant levels of drag reduction were reported using OSA even at the highest Reynolds number investigated, and because the corresponding actuation frequencies were relatively low, net power savings were projected to be possible in this regime.

Here, we extend this work by investigating drag reduction in an azimuthally oscillating turbulent pipe flow, in the absence of a traveling wave ($\kappa_x = 0$). A similar setup was used by Choi & Graham (1998), who studied Reynolds number up to $Re_\tau = 995$. In our experiment, we investigate a much wider range of Reynolds numbers, $856 < Re_\tau < 5744$. In addition, our experimental setup allows independent variation of Re_τ, T^+, and A^+, so that the scaling behavior of the drag reduction can be studied in detail.

As a result, we draw new conclusions regarding the scaling of drag reduction using TMI. Some of this work was reported by Ding *et al.* (2023), but here we present a detailed error analysis of the results, and discuss its implications on the drag reduction results. As a consequence, rather than making a distinction between the ISA and OSA regimes, we suggest instead that our data over the entire range of operating conditions collapses on a single scaling parameter $a^+ = A^+/T^+$ for all values of T^+ greater than about 100.

EXPERIMENTAL SETUP

Transverse momentum injection (TMI) is implemented by azimuthally oscillating a section of pipe housed within a recirculating water pipe facility. The recirculating pipe facility has an inner diameter ($D = 2R$) of 38.1 mm and maintains bulk flow velocities ranging from 1.1 to 4.2 m/s. The test section (depicted in figure 2) is a 1.22 m section of pipe placed more than $100D$ downstream of the inlet to ensure fully developed flow. This section of pipe is oscillated around its longitudinal axis using a crank-slider mechanism, where the length ratio of the crank to the rod-to-slider attachment is less than 0.05. This ensures oscillation closely approximates sinusoidal motion. The crank-slider mechanism utilizes symmetrical T-slot connections to permit manipulation of the amplitude of oscillation, and further translates the resulting linear motion to oscillatory motion via a timing belt. The frequency of oscillation is controlled and adjusted by a motor connected to the crank-slider mechanism via two additional timing belts.

Symmetry of the T-slot connections was essential to ensure stable operation at high frequencies and amplitudes of operation. Moreover, the motor-to-T-slot connection via two timing belts allows for equal distribution of forces between the symmetrical T-slots. This helps to mitigate potential failure of the T-slot mechanism. To ensure stable operation and reduce vibration of the test section, the natural frequency of the base table was also adjusted to frequencies outside our operating regime with the addition of both weights and table leg supports. The T-slot mechanism is further designed to allow for counterweight attachments when operating at maximum frequencies. This guarantees minimal vibration of the test section during high frequency operation.

Test Parameters

This experimental setup ensures a large range of available test parameters. The important parameters for this problem can be determined through dimensional analysis of the drag reduction mechanism depicted in figure 1, yielding the following relationship:

$$DR = DR(A^+, T^+, \kappa_x^+, Re_\tau) \tag{2}$$

where $A^+ = A/u_{\tau_0} = \omega d/u_{\tau_0}$, $T^+ = 2\pi u_{\tau_0}^2/(\omega\nu)$, and $\kappa_x^+ = \kappa_x \nu/u_{\tau_0}$. For azimuthal surface oscillations in pipe flow, d is the spanwise oscillation amplitude, and $u_{\tau_0} = \tau_{\omega_0}/\rho$ is the friction velocity of the non-oscillating reference case, where τ_{ω_0} is the time-averaged wall shear stress and ρ is the fluid density. Hence, $Re_\tau = u_{\tau_0} R/\nu$. In the absence of a streamwise traveling wave ($\kappa_x = 0$), the remaining test parameters are the non-dimensional velocity amplitude of oscillation (A^+), the non-dimensional period of oscillation (T^+), and the friction Reynolds number (Re_τ).

	Re_τ	A^+	T^+	$DR(\%)$
Experiment	649	1.76−22.1	608−48	0.5−24
(Choi & Graham, 1998)	995	2.37−17.2	663−91	0.8−22
DNS (Peet *et al.*, 2023)	720	10	100	22.9
Experiment	884 ± 28	7.83−30.2	472−130	3.3−30.6
(current data)	1343 ± 40	2.72−30.6	2019−176	0.0−28.1
	2224 ± 307	2.96−19.4	1672−439	0.7−10.2
	3970 ± 320	2.88−11.9	4203−1343	0.2−3.7
	5246 ± 498	3.59−8.33	6857−2084	0.0−2.2

Table 1. Scope of testing parameters and drag reduction results from existing experimental and numerical work for "fully turbulent" flow in an azimuthally oscillating pipe.

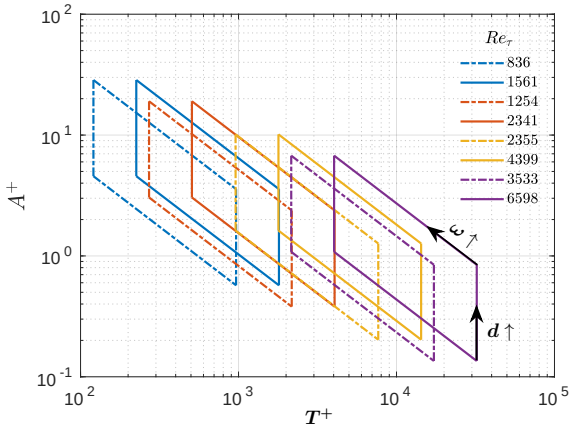

Figure 3. Achievable ranges of testing parameters. Each parallelogram indicates the range of (A^+, T^+) by varying ω and $d(\omega/(2\pi) \in [2, 16]$ Hz, $d \in [2, 12.8]$ mm) at fixed u_τ and ν (thus fixed Re_τ, as labeled in the legend). Each parallelograms pair of the same color represent the variation of Re_τ by changing only the water temperature (thus ν) from room temperature to about 57°C, and different colors are for different bulk velocity (thus u_τ) settings.

The ranges of Re_τ, A^+ and T^+ explored in this study are given in Table 1, and the achievable ranges of these parameters are graphically summarized in figure 3, in which different strategies for varying testing parameters are indicated. The T-slot mechanism depicted in figure 2 allows for manipulation of the oscillation amplitude up to d = 12.8 mm, where the motor controls the frequency of oscillation up to $f = \omega/(2\pi)$ = 20 Hz. Further, the recirculating pipe setup is attached to a water heater, allowing the flow to reach ambient temperatures up to 57°C. We are then able to control the temperature of the fluid (water) and the bulk flow speed to independently control Re_τ, while the T-slot and motor allow for significant independent variation in A^+ and T^+. In figure 3, each parallelogram represents the range of (A^+, T^+) with $2 < d < 12.8$ mm and $2 < f < 16$ Hz, when u_τ and ν are fixed. Each parallelogram pair of the same color defines the Re_τ range when u_τ (and bulk velocity) is fixed and ν is varied by changing water temperature from 20°C to 57°C; different colors are for Re_τ ranges by changing u_τ.

Pressure Measurements

Pressure taps were located 135 mm ($\approx 7R$) upstream and downstream of the rotating test section. The time-averaged pressure drop is then measured with a Validyne DP103 differential pressure sensor across these taps in the non-actuated and actuated cases. Drag reduction is then calculated as follows:

$$DR\% = (1 - \lambda/\lambda_0) \times 100 \tag{3}$$

Here, λ_0 is the friction factor for the non-actuated control case calculated from the friction factor correlation for smooth turbulent pipe flow given by McKeon *et al.* (2004). Pressure drop measurements taken across the test section in the non-actuated case (ΔP_0) are checked in-between actuated runs to ensure the pressure sensor accuracy. These control measurements are found to be within 1-2% of the pressure drops determined by the McKeon *et al.* (2004) correlation. This correlation is also used to determine u_{τ_0} for each test, where $\lambda_0 = 8u_{\tau_0}^2/U_b^2$.

The friction factor for the oscillating case (λ) is defined by $\lambda = -2\Delta PD/(L\rho U_b^2)$. Here L is the length of the oscillating test section, ρ is density, U_b is the bulk velocity of the flow, and ΔP is the pressure drop across the test section. We assume all drag alteration occurs within the oscillating section of pipe flow. Thus, in order to establish accurate drag reduction, we measure pressure drop across the pressure taps and subtract out the pressure drop in the upstream and downstream stationary pipe sections between the taps and the oscillating test section according to the McKeon *et al.* (2004) correlation.

For each combination of testing parameters, we acquire a minimum of 2,000 – 3,000 samples in the span of two or three trials. The sampling rate was approximately 5 Hz so that pressure measurements are not phase-locked with the pipe oscillation frequency. Two categories of contributions are considered for the uncertainty in our drag reduction measurements. The first category is the fluctuating part, capturing random measurement noise in the pressure sensor, turbulent fluctuations and phase-dependent fluctuations from the spanwise oscillation. The phase-dependent fluctuations are likely not significant – for example, Touber & Leschziner (2012) reported 1-2% phase dependent variations of DR at $Re_\tau = 500$. The combined contribution of this category is approximated as $\Delta p_{rms}/\sqrt{N_s}$, where Δp_{rms} is the root-mean-square pressure drop and N_s is the number of samples. This uncertainty never exceeds $\pm 0.2\%$ of the pressure drop in the trials collected. The second category of uncertainty is that due to the pressure sensor. The Vali-

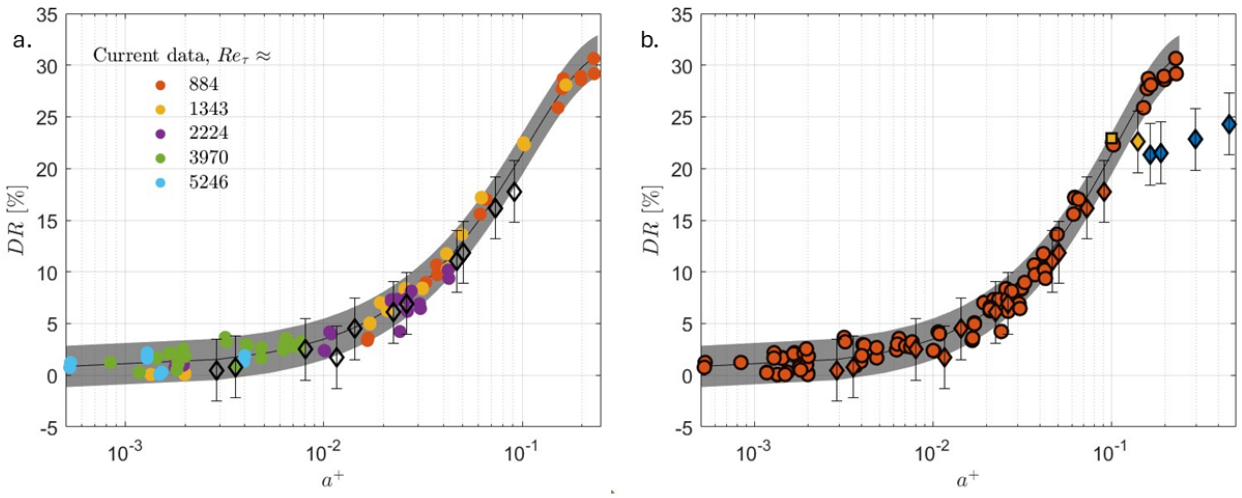

Figure 4. Drag reduction results against non-dimensional acceleration of oscillation ($a^+ = A^+/T^+$). a) Plots all tests where $T^+ > 100$. Filled circles represent current data color-coded by Re_τ in legend. This is plotted with Choi & Graham (1998) pipe flow data where $Re_\tau < 1000$, denoted by $\diamond$. b) Distinguishes sub-optimal frequencies ($T^+ < 100$) in blue, above-optimal frequencies ($T^+ > 100$) in red, and optimal frequency ($T^+ \approx 100$) in yellow. $\circ$ represent current data, $\diamond$ are pipe flow data from Choi & Graham (1998), and $\square$ is DNS from Peet *et al.* (2023). Line is provided for reference, with a $\pm 2\%$ error shaded region to represent experimental error in our current data. Choi & Graham (1998) error is given as $\pm 3\%$.

dyne DP103 allows for replaceable diaphragms, each with an accuracy of $\pm 0.5\%$ full scale pressure. The diaphragms were switched out to match the required full scale range and ensure maximum accuracy across the changing flow rates. The sensor was routinely calibrated, and the true zero offset was always monitored between tests. This category yields a maximum error of $\pm$1-2% when comparing to the McKeon *et al.* (2004) correlation. Therefore, we report $\pm 2\%$ uncertainty for all drag reduction data collected.

RESULTS

While the operating parameter space is much larger than that of previous TMI studies, restrictions within this space and the uncertainty in drag reduction measurement place limits on the full extent of the data set.

Limitations in High Re_τ Tests

From Table 1, we see a significant decrease in drag reduction at high Reynolds numbers, primarily because of the limitations on the values of A^+ and T^+ that could be achieved. These parameters depend on u_τ, i.e. $A^+ = \omega d/u_{\tau_0}$ and $T^+ = 2\pi u_{\tau_0}^2/(\omega\nu)$, and so higher frequencies and amplitudes of oscillation are required to maintain drag reducing values of A^+ and T^+. For example, as implied by figure 3, to achieve $T^+ < 500$ at $Re_\tau \approx 6600$ (the solid purple box), $f = \omega/(2\pi)$ needs to be about 130 Hz, whereas $f = 20$ Hz is practically the highest operation frequency of our set-up. The error analysis of our drag reduction data ($\pm 2\%$ error) then indicates that we were unable to measure the drag reduction for $Re_\tau \approx 4500$. While we are able to operate the recirculating pipe flow up to $Re_\tau \approx 7000$, we are limited by our maximum operating frequency and amplitude, both of which are too low to observe significant drag reduction in these flows.

Cut-off T^+

The drag reduction results are presented in figure 4 (see also Ding *et al.* (2023)). Notably, we observe a collapse of our drag reduction data against the parameter $a^+ = A^+/T^+$. This collapse follows for all data within our parameter space up to a maximum frequency, corresponding to a minimum non-dimensional period of oscillation , which we refer to as the cut-off period. The following discussion will review the sensitivity of this cut-off, and suggest that $T_c^+ \approx 100$.

From our experiments, we have results for $T^+ > 130$. All tests performed in this regime collapse with non-dimensional acceleration of oscillation (a^+), independent of Reynolds number, as shown in figure 4a, with a shaded region indicating $\pm 2\%$ error in the measurements.

Choi & Graham (1998) used a similar azimuthally oscillating pipe flow, but because there Reynolds numbers were significantly smaller ($Re_\tau < 995$) they achieved T^+ values as low as $T^+ \approx 50$. Their data, when plotted against non-dimensional acceleration of oscillation (a^+) for $T^+ > 100$, collapses alongside our data (see figure 4a). When $T^+ \leq 100$, however, this collapse no longer holds, as depicted in 4b. We conclude, therefore, that $T_c^+ \approx 100$, but because oscillation periods between 100 and 120 were not explored by Choi & Graham (1998), it may be that the cut-off lies somewhere within this range.

We can also use the recent DNS results for an azimuthally oscillating pipe obtained by Peet *et al.* (2023) at $T^+ = 100$. When plotted against a^+, this point collapses on the same curve as experimental data for $T^+ > 100$. This result further supports the conclusion that $T_c^+ \approx 100$.

Actuation at $T^+ \approx 100$ has been shown to be physically significant in many past studies of transverse momentum injection. Early DNS estimated the optimal period of oscillation to be at $T^+ \approx 100$ (Baron & Quadrio, 1995; Dhanak & Si, 1999); that is, the period of oscillation that optimizes the drag reduction. This is further supported in DNS by Blesbois *et al.* (2013), which found a streak amplification timescale of $t^+ = 50$. This result was later interpreted to mean that the

weakened streaks do not have enough time to regenerate if the oscillation changes direction every $t^+ = 50$ (Quadrio & Ricco, 2004).

As a result, most existing TMI work accepts $T^+ \approx 100$ as the optimal period of oscillation, though this has not been confirmed experimentally due to limitations in parameter space explored. In addition, there are several studies that suggest this optimal period of oscillation may decrease with increasing Reynolds number (Choi *et al.*, 2002; Yao *et al.*, 2019). This result has also yet to be confirmed.

CONCLUSIONS

This current study investigates drag reduction behavior in an azimuthally oscillating turbulent pipe flow at Reynolds numbers ranging from $Re_\tau \approx 856 - 5744$. A maximum drag reduction of 30.6% is reported. The outcome of this work further suggests that the key scaling parameter for this drag reduction behavior is the non-dimensional acceleration of the surface oscillation ($a^+ = A^+/T^+$), in accordance with the earlier work of Ding *et al.* (2023).

Our novel experimental setup, where the water temperature was varied allowing for independent variation of Re_τ, A^+, and T^+, permitted us to explore the scaling behavior of the drag reduction and demonstrate that the non-dimensional acceleration (a^+) is the key parameter, collapsing the data regardless of Re_τ, A^+.

An error analysis yielded a $\pm 2\%$ maximum error in the drag reduction measurements obtained. This error indicates that we are unable to measure significant drag reduction at $Re_\tau > 4500$ because it falls below the uncertainty level. Further expansion of the parameter space is required to determine drag reduction behavior at these higher Reynolds number values; however, the collapse of data against a^+ suggests that there is no Reynolds number dependence in this behavior.

The collapse of drag reduction data against the acceleration parameter is independent of Re_τ, A^+, and T^+; however, we are able to determine a cut-off period ($T_c^+ \approx 100$) below which this collapse no longer holds. We further note that $T^+ \approx 100$ is the period of oscillation in which the weakened streaks are unable to regenerate (Quadrio & Ricco, 2004), and is often assumed to be the optimal-period of oscillation in past TMI work.

REFERENCES

Baron, A. & Quadrio, M. 1995 Turbulent drag reduction by spanwise wall oscillations. *Applied Scientific Research* **55**, 311–326.

Bird, J., Santer, M. & Morrison, J.F. 2018 Experimental control of turbulent boundary layers with in-plane travelling waves. *Flow, Turbulence and Combustion* **100** (4), 1015–1035.

Blesbois, O., Chernyshenko, S., Touber, E. & Leschziner, M. 2013 Pattern prediction by linear analysis of turbulent flow with drag reduction by wall oscillation. *Journal of Fluid Mechanics* **724**, 607–641.

Choi, J. I., Xu, C.-X. & Sung, H. J. 2002 Drag reduction by spanwise wall oscillation in wall-bounded turbulent flows. *AIAA Journal* **40** (5), 842–850.

Choi, K. S., DeBisschop, J. R. & Clayton, B. R. 1998 Turbulent boundary-layer control by means of spanwise-wall oscillation. *AIAA Journal* **36** (7), 1157–1163.

Choi, K. S. & Graham, M. 1998 Drag reduction of turbulent pipe flows by circular-wall oscillation. *Physics of Fluids* **10** (1), 7–9.

Dhanak, M. R. & Si, C. 1999 On reduction of turbulent wall friction through spanwise wall oscillations. *Journal of Fluid Mechanics* **383**, 175–195.

Ding, L., Sabidussi, L., Holloway, B. C., Hultmark, M. & Smits, A. J. 2023 Acceleration is the key to drag reduction in turbulent flow. *arXiv preprint arXiv:2312.12591* .

Gatti, D. & Quadrio, M. 2013 Performance losses of drag-reducing spanwise forcing at moderate values of the reynolds number. *Physics of Fluids* **25** (12).

Gatti, D. & Quadrio, M. 2016 Reynolds-number dependence of turbulent skin-friction drag reduction induced by spanwise forcing. *Journal of Fluid Mechanics* **802**, 553–582.

Hurst, E., Yang, Q. & Chung, Y. M. 2014 The effect of reynolds number on turbulent drag reduction by streamwise travelling waves. *Journal of Fluid Mechanics* **759**, 28–55.

Lee, M. & Moser, R. D. 2015 Direct numerical simulation of turbulent channel flow up to $Re_\tau \approx 5200$. *Journal of Fluid Mechanics* **774**, 395–415.

Marusic, I., Chandran, D., Rouhi, A., Fu, M. K., Wine, D., Holloway, B., Chung, D. & Smits, A. J. 2021 An energy efficient pathway to turbulent drag reduction. *Nature Communications* **12** (1), 1–8.

McKeon, B. J., Swanson, C. J., Zagarola, M. V., Donnely, R. J. & Smits, A. J. 2004 Friction factors for smooth pipe flow. *Journal of Fluid Mechanics* **511**, 41–44.

Peet, Y., Coxe, D. & Adrian, R. 2023 Loss of effectiveness of transverse wall oscillations for drag reduction in pipe flows with Reynolds number. In *10th International Symposium on Turbulence, Heat and Mass Transfer, THMT 2023*. Begell House Inc.

Quadrio, M. & Ricco, P. 2004 Critical assessment of turbulent drag reduction through spanwise wall oscillations. *Journal of Fluid Mechanics* **521**, 251–271.

Quadrio, M., Ricco, P. & Viotti, C. 2009 Streamwise-travelling waves of spanwise wall velocity for turbulent drag reduction. *Journal of Fluid Mechanics* **627**, 161–178.

Touber, E. & Leschziner, M. A. 2012 Near-wall streak modification by spanwise oscillatory wall motion and drag-reduction mechanisms. *Journal of Fluid Mechanics* **693**, 150–200.

Wu, S. 2000 An investigation of the Reynolds number effect on drag reduction.

Yao, J., Chen, X. & Hussain, F. 2019 Reynolds number effect on drag control via spanwise wall oscillation in turbulent channel flows. *Physics of Fluids* **31** (08).